J|A|C|S
COMMUNICATIONS

Hydrogen-Bonded Ferroelectrics Based on Metal−Organic Coordination

Heng-Yun Ye,† Da-Wei Fu,† Yi Zhang,† Wen Zhang,† Ren-Gen Xiong,*,† and Songping D. Huang*,‡

Ordered Matter Science Research Center, Southeast University, Nanjing 211189, People's Republic of China, and Chemistry Department, Kent State University, Kent, Ohio 44240

Received October 23, 2008; E-mail: xiongrg@seu.edu.cn; shuang1@kent.edu

The properties of many compounds such as KDP (KH_2PO_4), ice (water), DNA, etc., depend on the specific features of hydrogen bonds (H-Bs). This looks like water composed of small H_2O molecules and like living tissues composed of huge biopolymers. The H-Bs can be considered donor−acceptor systems (the H atom is the acceptor, while N, O, and Cl are donors that provide a lone pair of electrons). Consequently, it displays directional but is much weaker than covalent bonds binding atoms into molecules. Thus, the aggregates created through H-Bs easily undergo transformations, induced by the breaking and formation of alternative H-Bs, proton transfers, or proton disordering. Such transformations can change the properties of crystals and enable the biopolymers to perform their living functions. A typical example for ferroelectrics through the H-B role is triglycine sulfate (TGS); it displays perfect hysteresis loop along the *b* axis, and its spontaneous polarization (P_s) reaches 3.5 $\mu C \cdot cm^{-2}$ at room temperature (rt).[1] The search for TGS-type hydrogen-bonded ferroelectrics has received relatively strong attention, in which Katrusiak et al. successfully explored rt ferroelectric dabcoHReO$_4$ (1,4-diazabicyclo[2.2.2]octane perrhenate or its perchlorate)[2] while Horiuchi et al. systematically investigated organic ferroelectrics through H-Bs at low temperature.[3] However, it is emphasized that their hysteresis loops look very nice and almost reach perfect P_s. The search for the ferroelectric metal−organic coordination (MOC) where its electric hysteresis loop is like them still remains a great challenge and is largely unexplored even though there are some Pervoskite-type ferroelectrics $[(CH_3)_3NH]_3[Sb_2Cl_9]$ [TMACA; where $(CH_3)_3NH$ is a trimethylammonium cation and $P_s = 2.0\ \mu C \cdot cm^{-2}$].[4] During exploration of potential ferroelectrics based on MOC,[5−18] we hardly have obtained one successful ferroelectrics example where its electric hysteresis loop reaches a perfect spontaneous polarization status, like that of TGS (as shown in Figure 3, in which we performed measurement of its electric hysteresis loop). Herein we report one MOC-type ferroelectric through H-Bs, cobalt(II) (*R*)-2-methylpiperazine (MPPA) trichloride $[Co^{II}Cl_3(H\text{-}MPPA)]$.

The reaction of a dichloride (*R*)-2-methylpiperazine bication with $CoCl_2$ affords an unexpected $[Co^{II}Cl_3(H\text{-}MPPA)]$ (as shown in Scheme 1 and Figures S1 and S2 in the Supporting Information) in which one of the N atoms is protonated while the other coordinates to the Co atom, proven by X-ray crystal structural determination later.[19]

Figure 1 clearly shows that the local coordination environment around the Co center can best be described as a distorted tetrahedron composed of three terminal Cl atoms and one N atom from an unprotonated N atom of MPPA. It is worth noting that one of the N atoms from the MPPA ligand is protonated and loses its coordination ability. Thus, three H atoms (H1, H2A, and H2B) form H-Bs between three Cl atoms (Cl1, Cl2, and Cl3) to lead to the formation of a 3D framework created through H-Bs (as shown in Figure 2a). A careful investigation shows that three bond distances of Co−Cl are not equal to each other and display some differences (D_{Co-Cl1} = 2.225 Å; D_{Co-Cl1} = 2.283 Å; D_{Co-Cl1} = 2.260 Å). As expected, the bond distance of Co1−N1 is in the normal range of Co−N bond lengths. Finally, the piperazine ring adopts a stable chair-type conformation as shown in Figure 1.

Scheme 1

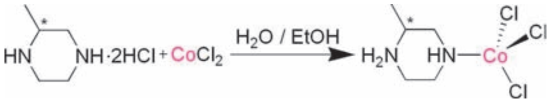

As $[Co^{II}Cl_3(H\text{-}MPPA)]$ crystallizes in chiral space group $P2_1$, which belongs to 1 of 10 polar point groups (C_2), its ferroelectric property will occur in principle. The single crystal with an approximate dimension of 0.40 × 0.35 × 0.26 mm was carefully selected with electrodes made of Cu wire with about 150 μm diameter covered by an Ag-conducting glue on the approximate crystallographic face (010). The electrodes were carefully amounted on a small six-pin dual-in-line IC socket under a microscope, and this supporter was connected on a ferroelectric tester. Figure 3 clearly shows that an electric hysteresis loop was observed when the applied electric field was set positive at about 20 kV from positive to negative voltage, showing that a spontaneous polarization ($P_s \approx 6.8\ \mu C \cdot cm^{-2}$) occurred in the measuring conditions and remanent polarization ($P_r \approx 6.2\ \mu C \cdot cm^{-2}$) was equal to almost that of P_s. For comparison, we measured the electric hysteresis loop of a TGS single crystal along the *b* axis at rt using the same measuring conditions as that of $[Co^{II}Cl_3(H\text{-}MPPA)]$. The result shows that a perfect electric hysteresis loop was recorded (inset in the right corner of Figure 3) and $P_s = 3.5\ \mu C \cdot cm^{-2}$ was detected. Thus, P_s of $[Co^{II}Cl_3(H\text{-}MPPA)]$ was as high as almost twice that of TGS and significantly larger than that of KDP at the low-

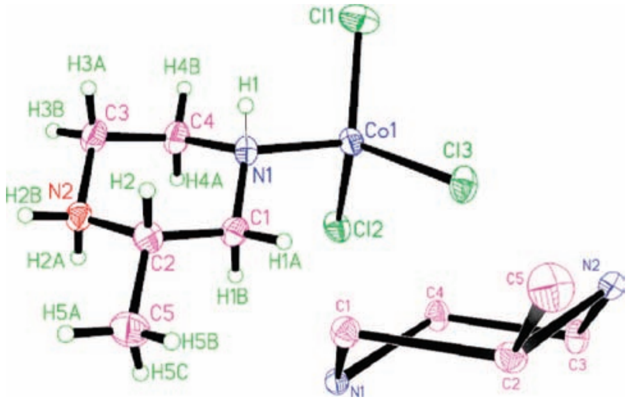

Figure 1. Molecular structure of the crystal state of $[CoCl_3(H\text{-}MPPA)]$ where the right corner is a chair conformation of a six-membered ring of the piperazine ring.

---

† Southeast University.
‡ Kent State University.

10.1021/ja808331g CCC: $40.75

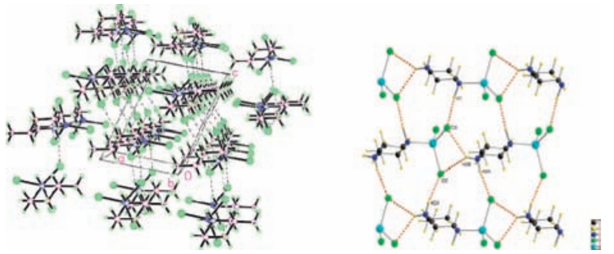

Figure 2. (a, left) Packing view along the *b* axis where a 3D framework is formed through H-Bs between H1, H2A, or H2B and CL1, Cl2, or Cl3. (b, right) Simple 2D network formed through Cl•••N H-Bs along the *b* axis. For details of the hydrogen bonds and angles, see Table S1 in the Supporting Information.

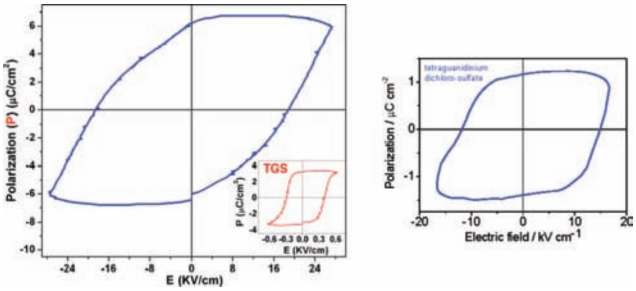

Figure 3. (a, left) Electric hysteresis loops are recorded on a Ferroelectric Tester Precision Premier II made by Radiant Technologies, Inc., at rt for [Co^{II}Cl$_3$(H-MPPA)] (the inset in the right corner is a typical TGS). (b, right) Loops for tetraguanidinium dichlorosulfate.[21]

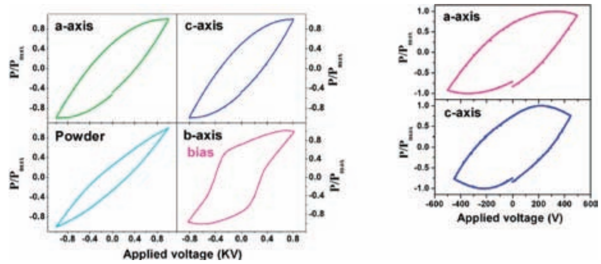

Figure 4. (a) Electric hysteresis loops in TGS (left). (b) Electric hysteresis loops for two other axes in [Co^{II}Cl$_3$(H-MPPA)].

temperature ferroelectric phase. As far as we know, [Co^{II}Cl$_3$(H-MPPA)] is the first example of ferroelectric MOC that can really reach the spontaneous polarization status, though there are lot of MOCs claimed to be ferroelectric compounds in which, however, their electric hysteresis loops never reach the spontaneous polarization status and only display a Chinese-cloth-maker-shuttle-like shape (also like the banana-shaped electric hysteresis loop pointed out by Scott[20]). On the other hand, it is very interesting to note that the electric hysteresis loop of powdered or single-crystal TGS along the *a* or *c* axis also shows banana-shaped loops (Figure 4) and never reaches the spontaneous polarization status. Sometimes, if we cut down the single crystals that are not perfectly parallel to the *b* face (010) of TGS, the electric hysteresis loop (an approximate square-wave loop) will become an approximate rhomb-wave loop, as depicted in Figure 4. Consequently, the loop (rhomb shape) of our case in [Co^{II}Cl$_3$(H-MPPA)] most likely occurs because the small single crystals are not perfectly cut down from along the *b* axis to lead to the a small mixture of crystal faces, and its shape looks like those found in tetraguanidinium dichlorosulfate[21] and dabcoHReO$_4$, in which their electric hysteresis loops also take after that of an ellipsoid (Figure 3b). The electric hysteresis loops along the *a* or *c* axis in [Co^{II}Cl$_3$(H-MPPA)] definitely look like a Chinese-cloth-maker-shuttle shape, as shown in Figure 4. Thus, we measured the dielectric constant of [Co^{II}Cl$_3$(H-MPPA)], showing that its value reaches the range of 26−22 along the *b* axis, which belongs to high dielectric compounds (see the Supporting Information). This further confirms that [Co^{II}Cl$_3$(H-MPPA)] is really ferroelectric.

The direction of the spontaneous polarization in the ferroelectric phase of [Co^{II}Cl$_3$(H-MPPA)] may be perpendicular to the chains and to the Cl•••HN H-Bs, analogically as in dabcoHReO$_4$, KDP, and other KDP-type ferroelectrics, where spontaneous polarization occurs nearly perpendicularly to the NH•••Cl H-Bs (Figure 2b). The mechanism leading to the ferroelectricity in [Co^{II}Cl$_3$(H-MPPA)] may pertain to most materials with bistable H-Bs such as dabcoHReO$_4$.[21]

An attempt to grow large crystals of [Co^{II}Cl$_3$(H-MP)] will soon be underway. In the present work, we have demonstrated that the MOC-based [Co^{II}Cl$_3$(H-MPPA)] containing H-Bs is a good ferroelectric candidate and opens up a new avenue to explore novel MOC-based ferroelectrics.

Acknowledgment. This work was supported by the NSFC, BK2008029 and 973 Project (Grant 2009CB623200).

Supporting Information Available: X-ray crystallographic CIF files, synthesis, XRD pattern, elementary analysis, the dielectric constant, the dc electric conductivity, the temperature dependence capacity, the measurements of TGA and DSC, the electric hysteresis loop, the crystal data for [Zn^{II}Cl$_3$(H-MPPA)], the piezoelectric coefficient d_{33}, and the details about hydrogen bonds and angles. This material is available free of charge via the Internet at http://pubs.acs.org.

References

(1) Matthias, B. T.; Miller, C. E.; Remeika, J. P. *Phys. Rev.* **1956**, *104*, 849.
(2) Szafrański, M.; Katrusiak, A.; McIntyre, G. J. *Phys. Rev. Lett.* **2002**, *89*, 215507–1.
(3) Horiuchi, S.; Tokura, Y. *Nat. Mater.* **2008**, *7*, 359.
(4) Jakubas, R.; Czapla, Z.; Galewski, Z.; Sobczyk, L. *Ferroelectrics Lett.* **1986**, *5*, 143.
(5) Zhang, W.; Xiong, R.-G.; Huang, S.-P. D. *J. Am. Chem. Soc.* **2008**, *130*, 10468.
(6) Fu, D.-W.; Ye, H.-Y.; Ye, Q.; Pan, K.-J.; Xiong, R.-G. *J. Chem. Soc., Dalton Trans.* **2008**, 874.
(7) Zhao, H.; Ye, Q.; Qu, Z.-R.; Fu, D. W.; Xiong, R.-G.; Huang, S.-P. D.; Chan, P. W. H. *Chem.—Eur. J.* **2008**, *14*, 1164.
(8) Ye, Q.; Fu, D.-W.; Tian, H.; Xiong, R.-G.; Chan, P. W. H.; Huang, S.-P. D. *Inorg. Chem.* **2008**, *47*, 772.
(9) Zhao, H.; Qu, Z.-R.; Ye, H.-Y.; Xiong, R.-G. *Chem. Soc. Rev.* **2008**, *37*, 84.
(10) Ye, Q.; Song, Y.-M.; Fu, D.-W.; Wang, G.-X.; Xiong, R.-G.; Chan, P. W. H.; Huang, S.-P. D. *Cryst. Growth Des.* **2007**, *7*, 1568.
(11) Gu, Z.-G.; Zhou, X.-H.; Jin, Y.-B.; Xiong, R.-G.; Zuo, J.-L.; You, X.-Z. *Inorg. Chem.* **2007**, *46*, 5462.
(12) Ye, Q.; Song, Y.-M.; Wang, G.-X.; Fu, D.-W.; Chen, K.; Chan, P. W. H.; Zhu, J.-S.; Huang, D. S.; Xiong, R.-G. *J. Am. Chem. Soc.* **2006**, *128*, 6554.
(13) Li, Y.-H.; Qu, Z.-R.; Zhao, H.; Ye, Q.; Xing, L.-X.; Wang, X.-S.; Xiong, R.-G.; You, X.-Z. *Inorg. Chem.* **2004**, *43*, 3768.
(14) Zhao, H.; Li, Y.-H.; Wang, X.-S.; Qu, Z.-R.; Wang, L.-Z.; Xiong, R.-G.; Abrahams, B. F.; Xue, Z.-L. *Chem.—Eur. J.* **2004**, *10*, 2386.
(15) Qu, Z.-R.; Zhao, H.; Wang, Y.-P.; Wang, X.-S.; Ye, Q.; Li, Y.-H.; Xiong, R.-G.; Abrahams, B. F.; Liu, Z.-G.; Xue, Z.-L.; You, X.-Z. *Chem.—Eur. J.* **2004**, *10*, 53.
(16) Xie, Y.-R.; Zhao, H.; Wang, X.-S.; Qu, Z.-R.; Xiong, R.-G.; Xue, X.-A.; Xue, Z.-L.; You, X.-Z. *Eur. J. Inorg. Chem.* **2003**, 3712.
(17) Zhao, H.; Qu, Z.-R.; Ye, Q.; Abrahams, B. F.; Wang, Y.-P.; Liu, Z.-G.; Xue, Z.-L.; Xiong, R.-G. *Chem. Mater.* **2003**, *15*, 4166.
(18) Qu, Z.-R.; Chen, Z.-F.; Zhang, J.; Xiong, R.-G.; Abrahams, B. F.; Xue, Z.-L. *Organometallics* **2003**, *22*, 2814.
(19) $C_5H_{13}Cl_3CoN_2$, $M_r = 266.45$, monoclinic, $P2_1$, $a = 7.020(3)$ Å, $b = 8.139(3)$ Å, $c = 9.731(4)$ Å, $\alpha = \gamma = 90°$, $\beta = 104.87(3)°$, $V = 537.4(4)$ Å^3, $Z = 2$, $D_c = 1.647$ Mg•m^{-3}, $R_1 = 0.0295$, $wR_2 = 0.0616$, $\mu = 2.288$ mm^{-1}, $S = 1.046$, Flack = 0.041(17).
(20) Scott, J. F. *J. Phys.: Condens. Matter* **2008**, *20*, 021001.
(21) (a) Szafrański, M. *Phys. Rev. B* **2005**, *72*, 054122. (b) Szafrański, M.; Katrusiak, A. *Phys. Rev. B* **2006**, *73*, 134111.

JA808331G